

# Chapter 1

## Introduction

### 1.1 Overview

An essential part to evaluate the success of global health is the access to appropriate diagnostic tools [1]. A commendable diagnostic tool should be able to identify the disease occurred from the individuals rapidly. Especially for the infectious diseases, the turnaround time (TAT) for the diagnosis strongly affects their exacerbation level to the community. In vitro diagnostic (IVD) tool is aimed to offer a comfortable diagnosis for the patients, by taking only small specimens from the human body, e.g., blood, urine, or sputum, for analysis. Consequently, technologies enabling effective in vitro diagnosis become highly attractive for both developed and developing countries [2]. Tremendous efforts have been geared toward developing clinical-level IVD tools. Despite achieving high accuracy, the resulting TAT can be too long for diagnoses of contagious diseases like Ebola and SARS in the rural area, and the requisite of skillful operators and sophisticated equipment to perform the assays can dramatically raise the cost of the assay.

Recently, decentralized diagnostic solutions, namely, point-of-care (PoC) devices, have gained notable interests attributed to their fastness, small footprint, and tiny sample usage. Wide varieties of diagnostic platforms have been invented, such as the lateral flow assays [3–6] and pathbreaking lab-on-a-disc immunoassay [7–10] for PoC applications. Beyond them, PoC devices on complementary metal–oxide–semiconductor (CMOS) chips are particularly promising, as they can enjoy the maturity of microelectronics in manufacturing and its outstanding performances in both physical sensing and signal processing. While the mainstream lateral flow assay is confounded to provide merely qualitative or semiquantitative results [11], the CMOS biosensors can attain a quantitative result and are beneficial to rapid and low-cost assays. Especially for low-cost IVD applications, CMOS chips in a centimeter scale can significantly miniaturize the diagnostic tools.

## 1.2 Global Necessities for In Vitro Diagnostic Tools

Decentralized healthcare systems are highly attractive for developing countries, as they typically suffer from lack of access to high-quality centralized diagnostic tools in the resource-limited area. Delay of diagnosis and treatment aggravates the healthcare condition of their countries, then affecting the global health system. According to the World Development Report in 2004, the lack of access results in failure of the health services [12]. Without proper equipment for diagnosis, the clinicians could only diagnose diseases from the clinical symptoms in resource-limited regions. Yet, this may cause difficulties in the diagnosis of the patients when the symptoms are still unobvious. Especially for infectious diseases, the delay of treatment can worsen the situation of individuals and consequently the communities. According to the report of the World Health Organization (WHO), the leading infectious diseases (lower respiratory infections, HIV/AIDS, diarrheal diseases, malaria, and tuberculosis) account for roughly one-third of all deaths in low-income countries [13]. Also, the strong growths of the population in those areas give rise to the demand of affordable IVD tools. By the end of 2050, the less developed countries are expected to have a population of 8.4 billion, as depicted in Fig. 1.1, where Africa and Asia contribute roughly 2.48 and 5.27 billion, respectively [14]. Thus, there is a rapidly growing market of low-cost PoC devices for developing countries.

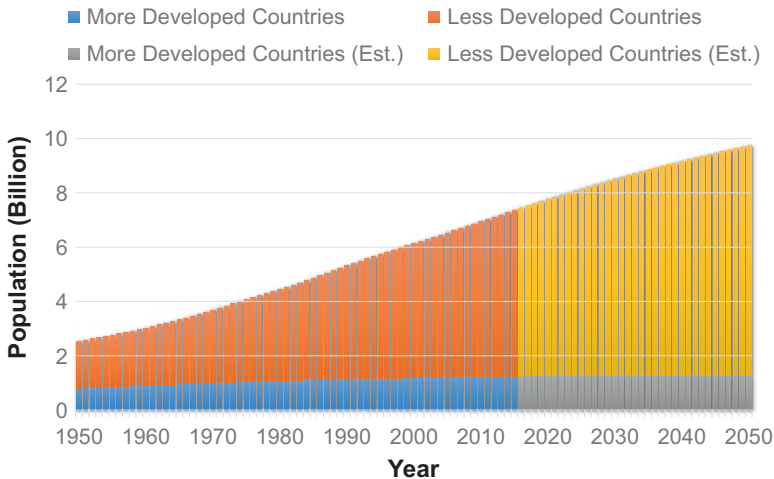


**Fig. 1.1** World population from 1950 to 2050, with a medium variant estimation from 2015. Data collected from the United Nations *World Population Prospects: The 2015 Revision* [14]. More developed countries: countries in Europe and Northern America, plus Australia/New Zealand and Japan. Less developed countries: countries in Africa, Asia (except Japan), Latin America, and the Caribbean plus Melanesia, Micronesia, and Polynesia

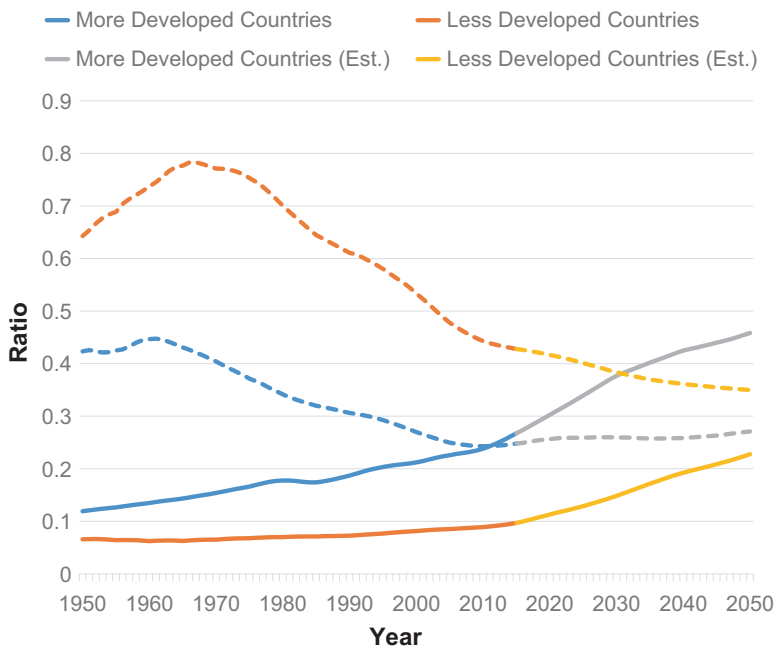


**Fig. 1.2** The old age dependency ratio (*solid line*), which is defined as the ratio of population of 65+ years old to the population of 15–64 years old with medium variant estimation from 2015. The children dependency ratio (*dotted line*), which is defined as the ratio of population of 0–14 years old to the population of 15–64 years old, is also shown on the graph as reference. Data collected from the United Nations *World Population Prospects: The 2015 Revision* [14]. More developed countries: countries in Europe and Northern America plus Australia/New Zealand and Japan. Less developed countries: countries in Africa, Asia (except Japan), Latin America, and the Caribbean plus Melanesia, Micronesia, and Polynesia

The aging problem of the developed countries also creates an enormous challenge. A healthcare solution that can deal with the continuous increment of life longevity is of demand. As revealed in Fig. 1.2, the old age dependency ratio, which gives insight to the population of elderly (65+ years) as a share of those in working age (age 15–64 years), will be rising in the coming decades. The old age dependency ratio of more developed countries will reach 0.4 in 2034 and eventually 0.46 by the end of 2050 (i.e., increase by 72% from 2015). Thus, the burdens on the clinical resources in those areas will become tighter, especially for the patients in proximity to death [15]. An efficacious healthcare solution will benefit this situation and drive the growth of the market for IVD tools. To this end, the market for IVD tools should not be merely aimed at less developing countries but also toward efficient and convenient diagnosis in developed countries. In fact, according to the report from Forbes/Investing, the IVD market, valued at ~\$50 billion in 2012, will expand to \$70 billion by 2017 [16].

### 1.3 Nuclear Magnetic Resonance for In Vitro Diagnosis

Nuclear magnetic resonance (NMR) is powerful to explore the sample information at the molecular level. The underpinning physics of NMR is the exchange of energy between the RF magnetic field and the spin of the non-zero spin nuclei (i.e.,  $^1\text{H}$ ,  $^{13}\text{C}$ ,  $^{17}\text{O}$ ,  $^{31}\text{P}$ , etc.) [17, 18]. Under the magnetization with an external magnetic field  $B_0$ , parts of the nuclei align with this external magnetic field and have a spin-up state, while the others have a spin-down state and align in opposite direction (Fig. 1.3a). As the population ratio between the nuclei with spin-up and spin-down state is proportional to  $B_0$  and this difference determines the amplitude of the NMR signal, there exists a tradeoff between the portability and sensitivity of the system as discussed later. With an RF magnetic field  $B_1$  orthogonal to  $B_0$  applied to the nuclei, they precess and tip away from the direction of bulk magnetization (Fig. 1.3b). The nuclei only accept RF excitation at Larmor frequency, defined as:

$$f_L = \gamma B_0 \quad (1.1)$$

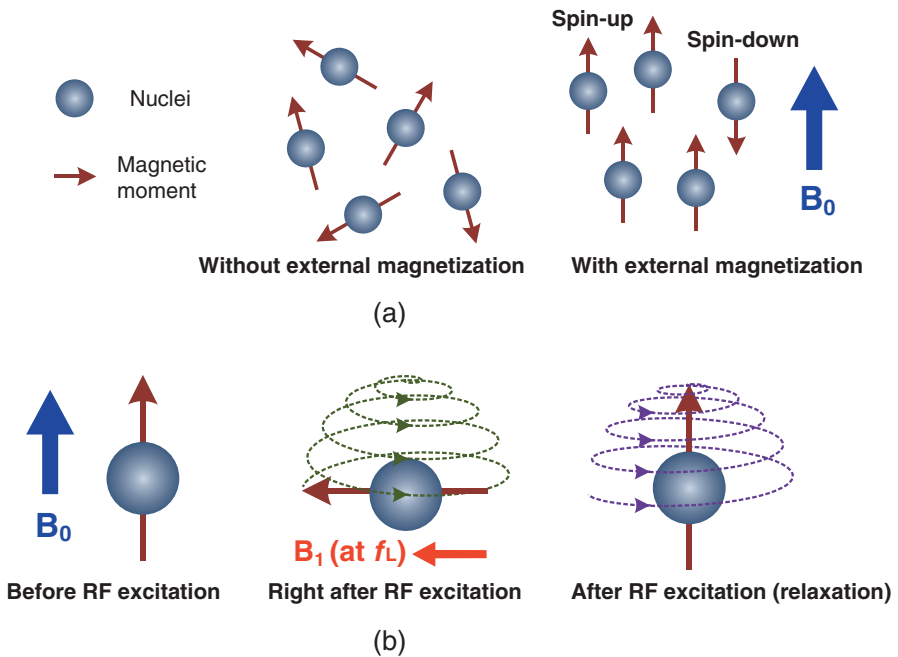


**Fig. 1.3** (a) Macroscopic view of the non-zero spin nuclei. With an external magnetic field  $B_0$  applied to the nuclei, part of them will align with this magnetic field. (b) The effect of RF excitation on the nucleus under external magnetization. When excited by the RF magnetic field at  $f_L$ , the nuclei precess around the magnetization. After this excitation, the nuclei still resonate and return to the equilibrium, with this relaxation recorded and analyzed

with the gyromagnetic ratio of the nuclei  $\gamma$ . For a 0.46-T magnet, the  $f_L$  of  $^1\text{H}$  is  $\sim 20$  MHz. The nuclei do not precess if there is a mismatch on the excitation frequency and  $f_L$ . After tipping the nuclei with  $90^\circ$  from the direction of bulk magnetization, the excitation is turned off. Then, the recovery of the magnetization in parallel with  $B_0$  is defined as the spin-lattice relaxation time  $T_1$  whereas the recovery of the magnetization perpendicular with  $B_0$  is defined as the spin-spin relaxation time  $T_2$ . This  $T_2$  reveals the magnetic field decoherence information across the nuclei. Unfortunately, the unavoidable inhomogeneity of  $B_0$  from portable magnet causes spatial variation on the precession rate of the nuclei thus the  $T_2$  decays at a much faster rate  $T_2^*$ . This blemish hinders the measurement on original  $T_2$ . To surmount this, the spin-echo technique such as Carr–Purcell–Meiboom–Gill (CPMG) pulse sequence can be utilized to refocus this dephasing effect on the nuclei by flipping the nuclei  $180^\circ$  with interval  $\tau$ ; thus the spins are maximized again from  $B_0$  inhomogeneity [19, 20]. The envelope of the echoes responses allows the derivation of the resulting  $T_2$  with the following mathematical expression:

$$A[n] = A_0 e^{-\frac{n\tau}{T_2}} \quad (1.2)$$

with the echoes amplitude for  $n$ th echoes  $A[n]$  and the initial amplitude  $A_0$ . More importantly, the strength of  $B_0$  correlates to the signal-to-noise ratio (SNR) of the NMR signal and is described as [21]:

$$\text{SNR}_{\text{NMR}} \propto KB_1 \sqrt{\frac{1}{Fl\xi\Delta f}} \left(\frac{f_L}{2\pi}\right)^{\frac{7}{4}} \frac{1}{\sqrt[4]{\rho}} \quad (1.3)$$

with homogeneity factor  $K$ , magnetic field strength per unit current produced by the RF-coil orthogonal to the permanent magnetic field  $B_1$ , the noise figure of the receiver's forefront amplifier  $F$ , length of the RF-coil conductor  $l$ , the bandwidth of the system  $\Delta f$ , and the resistivity  $\rho$  of the RF coil. From (1.1) and (1.3), the SNR of the system is proportional to the power of  $7/4$  of  $B_0$ , thus demanding a stronger  $B_0$  to enhance the SNR. Although there seem to be numerous ways to enhance  $B_0$  and its homogeneity (i.e., for higher resolution and stronger signal), the portability and power consumption of the system will be penalized due to the need for a heavier and bulkier magnet, not to mention a higher operating frequency that will be required for the electronics.

By exploiting functionalized magnetic nanoparticles (MNPs) as the probe, the NMR-based quasi label-free detection scheme can pinpoint a broad range of unprocessed biological targets such as DNA [22], protein [23], and virus [24] for in vitro diagnosis. These superparamagnetic MNPs have significant impacts on  $T_2$  of the samples according to their magnetization ( $M_s$ ) attributed to their capability to perturb the local magnetic field homogeneity. When the target is absent in the sample, the MNPs stay monodisperse inside the solution (Fig. 1.4a). Consequently, when

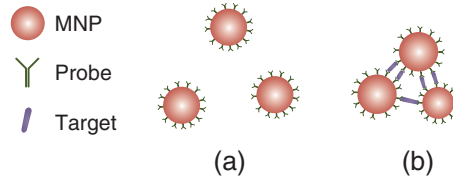


**Fig. 1.4** The state of the probe-functionalized MNPs. (a) Without the target, the MNPs stay monodisperse in the solution without any aggregation. (b) When the targets exist in the sample, the targets bind with the probe, and the MNPs aggregate to form micro-clusters

the targets exist inside the samples, they will cross-link with the probe-functionalized MNPs, assembling nanoparticles micro-clusters (Fig. 1.4b). These micro-clusters, with a diameter  $d_c$  depending on the concentration of the target biomolecules, have a different magnetization  $M_c$  [25]:

$$M_c = M_s \left( \frac{d_c}{d_s} \right)^{f-3} \quad (1.4)$$

with the fractal dimension of the micro-cluster  $f$  and the diameter of a single MNP  $d_s$ . Accordingly,  $T_2$  of the sample is commensurate with  $M_c$ . In this respect,  $T_2$  is linked with the amount of target upon nanoparticle agglomeration and attainable for quantification. Unlike other sensing schemes, screening by NMR is rapid and low cost as it is quasi label-free for the samples and immobilization-free for the transducers/electrodes. Such benefits render NMR-based detection as a promising solution for PoC applications. Although NMR is known for its relatively low sensitivity, the MNP here provides inherent signal amplification to NMR since a single MNP micro-cluster can affect billions of adjacent water molecules [26].

Conventionally NMR equipment are bulky and have limited applicability for PoC diagnosis. Recently, researchers have been focusing on miniaturizing the magnet for NMR and migrating the modular and complex electronics into CMOS chips [27–29]. With advanced circuit techniques to lessen the penalty of signal attenuation induced by the compact magnet (<7.3 kg) as stated in (1.3), these micro-NMR systems offer a trailblazing sensing method befitting more the PoC diagnosis.

## 1.4 Organization

The book is organized as below:

Chapter 2 reviews the state-of-the-art CMOS biosensors for in vitro diagnosis [30]. The first session focuses on introducing different transducing mechanisms for CMOS biosensors. According to the transducing mechanism, the CMOS biosensors can be categorized into electrical based, optical based, magnetic based, mechanical based, and NMR based. In the second session, in vitro diagnosis on different bio-

logical targets with CMOS biosensors and their applications is discussed. Subsequently, the strengths and weaknesses of different sensing mechanisms for these biosensors are compared in detail.

Chapter 3 illustrates the design and implementation of the palm-size micro-NMR relaxometer with the electronic-automated digital microfluidic device for sample management. Confounded by the limited inner space of the portable magnet, management of the sample under assay remains a critical issue for micro-NMR. Herein the integration of micro-NMR with the digital microfluidic device is evinced to facilitate the sample management and attain a comparable assay result to the conventional approach [31–35].

Chapter 4 discloses the design of the micro-NMR relaxometer with  $B_0$ -field stabilization module [36, 37]. Ascribed to the temperature instability of the magnet, calibration on either excitation frequency or Larmor frequency of the protons is necessary to safeguard the operation of the micro-NMR relaxometer. Herein, a vertical Hall sensor and relevant readout circuit are integrated with the micro-NMR transceiver to sense the  $B_0$ -field variation of the magnet for calibrating the  $B_0$  field of the portable magnet by injecting a current to its auxiliary coil. The closed-loop  $B_0$ -field stabilization here can suppress the variation of the  $B_0$  field and ease the operation.

Finally, Chap. 5 concludes the book and discusses the potential future works.

## References

1. D.C.H. Burgess, J. Wasseramn, C.A. Dahl, Global health diagnostics. *Nature* (suppl. 1) **444**, 1–2 (2006)
2. P. Yager, G.J. Domingo, J. Gerdes, Point-of-care diagnostics for global health. *Annu. Rev. Biomed. Eng.* **10**(1), 107–144 (2008)
3. M. Zuiderwijk, H.J. Tanke, R. Sam Niedbala, P.L.A.M. Corstjens, An amplification-free hybridization-based DNA assay to detect *Streptococcus pneumoniae* utilizing the up-converting phosphor technology. *Clin. Biochem.* **36**(5), 401–403 (2003)
4. X. Fu, Z. Cheng, J. Yu, P. Choo, L. Chen, J. Choo, A SERS-based lateral flow assay biosensor for highly sensitive detection of HIV-1 DNA. *Biosens. Bioelectron.* **78**, 530–537 (2016)
5. J. Li, J. Macdonald, Multiplex lateral flow detection and binary encoding enables a molecular colorimetric 7-segment display. *Lab Chip* **16**(2), 242–245 (2016)
6. J.R. Choi, J. Hu, R. Tang, Y. Gong, S. Feng, H. Ren, et al., An integrated paper-based sample-to-answer biosensor for nucleic acid testing at the point of care. *Lab Chip* **16**(3), 611–621 (2016)
7. M. La, S.M. Park, D.S. Kim, Centrifugal multiplexing fixed-volume dispenser on a plastic lab-on-a-disk for parallel biochemical single-end-point assays. *Biomicrofluidics* **9**(1), 014104 (2015)
8. B.S. Lee, Y.U. Lee, H.-S. Kim, T.-H. Kim, J. Park, J.-G. Lee, et al., Fully integrated lab-on-a-disc for simultaneous analysis of biochemistry and immunoassay from whole blood. *Lab Chip* **11**(1), 70–78 (2011)
9. J. Park, V. Sunkara, T.-H. Kim, H. Hwang, Y.-K. Cho, Lab-on-a-disc for fully integrated multiplex immunoassays. *Anal. Chem.* **84**(5), 2133–2140 (2012)
10. W.S. Lee, V. Sunkara, J.-R. Han, Y.-S. Park, Y.-K. Cho, Electrospun TiO<sub>2</sub> nanofiber integrated lab-on-a-disc for ultrasensitive protein detection from whole blood. *Lab Chip* **15**(2), 478–485 (2015)

11. G.A. Posthuma-Trumpie, J. Korf, A. van Amerongen, Lateral flow (immuno)assay: its strengths, weaknesses, opportunities and threats. A literature survey. *Anal. Bioanal. Chem.* **393**(2), 569–582 (2009)
12. *World development report: making services work for poor people* (World Bank, New York, 2004)
13. *The top 10 causes of death*, Available: <http://www.who.int/mediacentre/factsheets/fs310/en/index2.html>. Accessed 10 June 2016
14. *World population prospects: the 2015 revision* (United Nations, New York, 2015)
15. A. Palangkaraya, J. Yong, Population ageing and its implications on aggregate health care demand: empirical evidence from 22 OECD countries. *Int. J. Health Care Finance Econ.* **9**(4), 391–402 (2009)
16. Z. Miller, *Investing in the future of medicine: a investor's guide to the in vitro diagnostics market*, Available: <http://www.forbes.com/sites/zackmiller/2014/02/12/investing-in-the-future-of-medicine-a-investors-guide-to-the-in-vitro-diagnostics-market/#9d6e5ea5feb4>. Accessed 10 June 2016
17. B. Cowan, *Nuclear magnetic resonance and relaxation* (Cambridge University Press, Cambridge, 1997)
18. N.E. Jacobsen, *NMR spectroscopy explained: simplified theory, applications and examples for organic chemistry and structural biology* (Wiley, Hoboken, 2007)
19. H.Y. Carr, E.M. Purcell, Effects of diffusion on free precession in nuclear magnetic resonance experiments. *Phys. Rev.* **94**(3), 630–638 (1954)
20. S. Meiboom, D. Gill, Modified spin-echo method for measuring nuclear relaxation times. *Rev. Sci. Instrum.* **29**(8), 688–691 (1958)
21. D.I. Hoult, R.E. Richards, The signal-to-noise ratio of the nuclear magnetic resonance experiment. *J. Magn. Reson.* **24**(1), 71–85 (1976)
22. L. Josephson, J.M. Perez, R. Weissleder, Magnetic nanosensors for the detection of oligonucleotide sequences. *Angew. Chem.* **113**(17), 3304–3306 (2001)
23. J.M. Perez, L. Josephson, T. O'Loughlin, D. Hogemann, R. Weissleder, Magnetic relaxation switches capable of sensing molecular interactions. *Nat. Biotechnol.* **20**(8), 816–820 (2002)
24. J.M. Perez, F.J. Simeone, Y. Saeki, L. Josephson, R. Weissleder, Viral-induced self-assembly of magnetic nanoparticles allows the detection of viral particles in biological media. *J. Am. Chem. Soc.* **125**(34), 10192–10193 (2003)
25. C. Min, H.L. Shao, M. Liang, T.J. Yoon, R. Weissleder, H. Lee, Mechanism of magnetic relaxation switching sensing. *ACS Nano* **6**(8), 6821–6828 (2012)
26. H. Lee, E. Sun, D. Ham, R. Weissleder, Chip-NMR biosensor for detection and molecular analysis of cells. *Nat. Med.* **14**(8), 869–874 (2008)
27. N. Sun, Y. Liu, H. Lee, R. Weissleder, D. Ham, CMOS RF biosensor utilizing nuclear magnetic resonance. *IEEE J. Solid State Circuits* **44**(5), 1629–1643 (2009)
28. N. Sun, T.J. Yoon, H. Lee, W. Andress, R. Weissleder, D. Ham, Palm NMR and 1-Chip NMR. *IEEE J. Solid State Circuits* **46**(1), 342–352 (2011)
29. D. Ha, J. Paulsen, N. Sun, Y.Q. Song, D. Ham, Scalable NMR spectroscopy with semiconductor chips. *Proc. Nat. Acad. Sci. (PNAS)* **111**(33), 11955–11960 (2014)
30. K.-M. Lei, P.-I. Mak, M.-K. Law, R.P. Martins, CMOS biosensors for *in vitro* diagnosis – transducing mechanisms and applications. *Lab Chip* **16**(19), 3664–3681 (2016)
31. K.-M. Lei, P.-I. Mak, M.-K. Law, R.P. Martins, NMR–DMF: a modular nuclear magnetic resonance–digital microfluidics system for biological assays. *Analyst* **139**(23), 6204–6213 (2014)
32. K.-M. Lei, P.-I. Mak, M.-K. Law, R.P. Martins, A thermal-insensitive all-electronic modular  $\mu$ NMR relaxometer with a 2D digital microfluidic chip for sample management, in *Proceeding 19th International Conference on Miniaturized System Chemistry and Life Science (MicroTAS)*, 2015, pp. 302–304
33. K.-M. Lei, P.-I. Mak, M.-K. Law, R.P. Martins, A  $\mu$ NMR CMOS transceiver using a Butterfly-coil input for integration with a digital microfluidic device inside a portable magnet, in *Proceeding IEEE Asian Solid-State Circuits Conference (A-SSCC)*, 2015, pp. 1–4



34. K.-M. Lei, P.-I. Mak, M.-K. Law, R.P. Martins, A palm-size  $\mu$ NMR relaxometer using a digital microfluidic device and a semiconductor transceiver for chemical/biological diagnosis. *Analyst* **140**(15), 5129–5137 (2015)
35. K.-M. Lei, P.-I. Mak, M.-K. Law, R.P. Martins, A  $\mu$ NMR CMOS transceiver using a Butterfly-coil input for integration with a digital microfluidic device inside a portable magnet. *IEEE J. Solid State Circuits* **51**(10), 2274–2286 (2016)
36. K.-M. Lei, H. Heidari, P.-I. Mak, M.-K. Law, F. Maloberti, R.P. Martins, A handheld 50pM-sensitivity micro-NMR CMOS platform with B-field stabilization for multi-type biological/chemical assays, in *IEEE International Solid-State Circuits Conference Digest of Technical Papers (ISSCC)*, 2016, pp. 474–475
37. K.-M. Lei, H. Heidari, P.-I. Mak, M.-K. Law, F. Maloberti, R.P. Martins, A handheld high-sensitivity micro-NMR CMOS platform with B-Field stabilization for multi-type biological/chemical assays. *IEEE J. Solid State Circuits* **52**(1), 284–297 (2017)